Available online at www.sciencedirect.com

SciVerse ScienceDirect

Ceramics International 38 (2012) 6137–6144

CERAMICS INTERNATIONAL

www.elsevier.com/locate/ceramint

Microstructure and tribological behaviors of C/C–BN composites fabricated by chemical vapor infiltration

Xiaomeng Fan, Xiaowei Yin*, Yu Cheng, Litong Zhang, Laifei Cheng

Science and Technology on Thermostructural Composite Materials Laboratory, Northwestern Polytechnical University, Xi'an, Shaanxi 710072, PR China

Received 29 February 2012; received in revised form 19 April 2012; accepted 26 April 2012
Available online 11 May 2012

Abstract

In this paper carbon fiber reinforced carbon–boron nitride binary matrix composites (C/C–BN) were prepared by chemical vapor infiltration (CVI). The infiltration of BN in the CVI process was controlled by the diffusion of BCl_3, and BN matrix was distributed homogeneously in the porous carbon fiber reinforced carbon matrix composites (C/C) due to the good infiltration ability of BN. The as-received C/C–BN composites were composed of 92 vol% C and 8 vol% BN. Both the friction coefficient and wear rate of C/C composites decreased significantly by the incorporation of BN. After heat-treated at 1600 °C, the interlayer spacing of CVI BN decreased to 3.36 Å, and CVI BN with high crystalline degree displayed the excellent lubricating effect, leading to the decrease of friction coefficient and wear rate. The improvement of the tribological properties also was partially attributed to the improved oxidation resistance and the formation of friction film by the incorporation of BN matrix.

Keywords: C. Friction; C. Wear resistance; Boron nitride; CVI

1. Introduction

Carbon fiber reinforced carbon matrix composites (C/C) are one of the most promising candidate materials for high-temperature applications because of their intrinsic high thermal stability and low density [1–6]. Based on the research of C/C composites, many works are carried out to modify the properties of C/C composites to further extend their application field [7–11]. The incorporation of SiC in the C/C composites is an effective way to improve their tribological behaviors, and carbon fiber reinforced C–SiC binary matrix composites (C/C–SiC) fabricated by liquid silicon infiltration (LSI) have been widely researched and successfully applied as braking materials at high-speed braking field [12–18]. However, C/C composites with low friction coefficient and low wear rate are required for the potential application in the field of sealing materials and sliding element at high temperatures [1,19]. In order to decrease the friction coefficient and wear rate effectively, the lubricating additive is introduced into the C/C composites in the present work.

Hexagonal boron nitride (h-BN) has the similar laminate structure like graphite, and also has many similar properties and uses [20]. It has a low hardness (Mohs hardness 1∼2), high thermostability, and better oxidation resistance than graphite [21]. Owing to the weak Van Der Walls force between each layer, h-BN is easily sheared along the basal plane of hexagonal crystalline structure, leading to the excellent lubricating performance of BN [22]. The friction coefficient for Si_3N_4 containing 30 vol% BN against stainless steel reached 0.03 [23], and the friction coefficient of sliding bearings lubricated by the mixture of BN and oil reached as low as 0.015 [24], which all displayed the outstanding lubricating performance of BN.

BN has been introduced into C/C composites by polymer infiltration and pyrolysis (PIP), and carbon fiber reinforced C–BN binary matrix composites (C/C-BN) fabricated by PIP displayed better wear resistance than C/C composites [25,26]. Besides PIP, chemical vapor infiltration (CVI) is another promising process to fabricate

*Corresponding author. Tel.: +86 29 88494947; fax: +86 29 88494620.
E-mail addresses: yinxw@nwpu.edu.cn, fanxiaomeng@163.com (X. Yin).

0272-8842/$36.00
http://dx.doi.org/10.1016/j.ceramint.2012.04.063

ceramic matrix composites. The CVI method has various advantages [27,28]: (1) the process can be conducted at low pressure and low temperature, no external pressure is required, so fiber reinforced ceramic matrix composites with high performance can be fabricated owing to the small residual stress and less damage on the fiber; (2) the phase composition of the matrix can be easily designed by adjusting the kind, concentration, and deposition sequence of the reaction gases; (3) the components with complex shape and high volume content of fibers can be fabricated by a near-net shape process.

However, no literature about C/C–BN composites fabricated by CVI can be found up to now. Therefore, BN was introduced into the C/C composites by CVI to obtain BN modified C/C composites with low friction coefficient and low wear rate in the present work.

In our previous work [29], the microstructure and deposition kinetic of CVI BN were studied, as well as the crystallization degrees of BN annealed at different temperature. In this paper, C/C–BN composites were prepared by CVI, and then the microstructures and tribological behaviors of C/C–BN composites were investigated in comparison with those of C/C and C/C–SiC composites.

2. Experimental

2.1. Fabrication procedure of samples

In this paper, the 3D needled integrated felts with a density of 0.55 g/cm^3 and a fiber volume fraction of 32% were used as the preform. All the carbon types were PAN-based carbon fiber (T300, 12 K, Toray, Japan). The needled integrated felts were fabricated by repeatedly overlapping the layer of 0° non-woven fiber cloth, short-cut fiber cloth and 90° non-woven fiber cloth with needled-punching step by step. The 3D needled carbon fiber preforms were infiltrated by low pressure chemical vapor infiltration (CVI) in a mixture of C_3H_6 and Ar atmosphere to form C/C composites.

For C/C–BN composites, BN matrix was introduced into the porous C/C composites by CVI for 40 h in a vertical hot-wall reaction furnace with a total pressure of 1000 Pa at 1000 °C. The fluxes of inlet gas were selected as follows: BCl_3 = 20 ml/min, NH_3 = 60 ml/min, Ar = 50 ml/min and H_2 = 100 ml/min. The as-received C/C–BN composites were heat-treated at 1600 °C in nitrogen atmosphere for 2 h. After heat-treated at 1600 °C, the interlayer spacing of CVI BN decreased to 3.36 Å [29], which was lower than that of CVI BN heat-treated at lower temperature. The smaller interlayer spacing of BN means the stronger atomic bonding, leading to the higher moisture resistance. When the CVI BN heat-treated at 1600 °C was exposed to 50 vol% H_2O/50 vol% Ar atmosphere at 700 °C for 10 h, the sample had no weight variation owing to the good moisture resistance of CVI BN heat-treated at 1600 °C.

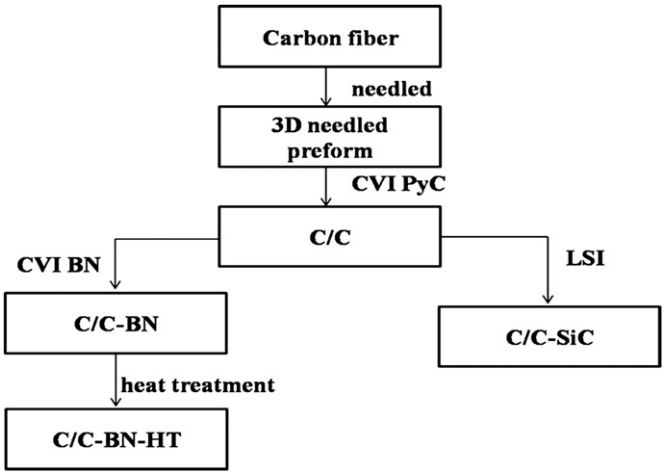

Fig. 1. The schematic of the fabrication procedures of composites.

For C/C–SiC composites, the porous C/C composites were infiltrated with liquid silicon directly in a vacuum furnace at 1500 °C for 0.5 h, and a dense material was obtained. The manufacturing process of composites is presented in Fig. 1. The infiltration of silicon in the carbon material during LSI process has been discussed in the previous literatures [30,31], and the liquid silicon infiltrated the porous composites spontaneously by the capillary force [32], so no detailed discussion on the infiltration ability of liquid silicon in the porous C/C composites appears in this paper.

2.2. Friction and wear test

Friction and wear properties of all the samples were performed on a disk-on-disk MM-1000 testing machine. The tests were carried out with a rotating disk of Φ76 mm × Φ52 mm × 12 mm (76 mm in outer diameter, 52 mm in inner diameter and 12 mm in thickness) and a stationary disk of Φ90 mm × Φ55 mm × 12 mm. Braking test was performed under a moment of inertia of 0.235 kg m^2 with a braking speed of 28 m/s and a braking pressure of 0.8 MPa. Each braking test was repeated for 20 times under the same braking condition. The weight wear rate was calculated by measuring the weight of disks before and after braking tests divided by total number of braking tests. The friction coefficient is calculated using Eq. (1).

$$M = \mu(r_1 + r_2)P/2 \quad (1)$$

where M is the moment, μ is the friction coefficient, P is the braking pressure, r_1 is the inner radius and r_2 is the outer radius.

2.3. Characterizations

Phase analysis was conducted by X-Ray Diffraction (XRD), via a computer-controlled diffractometer (X'Pert Pro, Philips, Netherlands) with CuKα radiation at 40 kV and 100 mA. Data was digitally recorded in a continuous

scanning mode in the angle (2θ) ranging from 10° to 80 with a scanning rate of 0.12°/s. The pore size distribution was measured using a Mercury Porosimeter (Poremaster 33, Quantachrome Instruments Corporation, Boynton Beach, FL, USA). The optical microstructure of C/C composites was observed by a polarized light microscope (PLM, Leica DLMP, Germany). The microstructure of the composites and wear debris were observed by a scanning electron microscope (SEM, S-2700, Hitachi, Japan) at 15 kV and 10 mA. The morphology of the worn surface of disks was observed by an optical microscopy (OM, Leica DLMP, Germany).

3. Results and discussion

3.1. Microstructure and pore size distribution of C/C composites

The density and open porosity of the 3D needled C/C composites were 1.50 g/cm^3 and 25%, respectively. Fig. 2 presents the typical microstructure of C/C composites. As shown in Fig. 2, a carbon matrix layer was formed around the carbon fiber, and the intra-bundle pores in the non-web cloth were well infiltrated, while the inter-bundle pores with large size remained in the short-web fiber cloth. By the polarized light, C/C composites showed rough laminar structure (RL) (Fig. 2c), which displayed high optical anisotropy. As known from Fig. 3, the pore size of C/C composites varied from 10 μm to 100 μm due to the existence of the inter-bundle pore.

3.2. Infiltration ability analysis of CVI BN in C/C composites

In the CVI process, the infiltration ability of BN is important to the fabrication of C/C–BN composites. CVI is a reaction-diffusion competition process. The typical CVI procedure is as follows: (1) gaseous reactants enter the reaction chamber; (2) the gaseous reactants diffuse into the inner of the preform through open pores and react with each other; (3) the solid reaction products deposit on the wall of the pores, and the gaseous byproducts diffuse out from the open pores; and (4) the unreacted gaseous reactants and byproducts exit from the reaction chamber. The gaseous diffusion in the porous preform is divided into three modes: Fick diffusion, Knudsen diffusion and transition diffusion. The diffusion mode is determined by the Knudsen number, K_n [33,34]:

$$k_n = \lambda_0/d \quad (2)$$

where λ_0 is the mean free path, and d is the mean pore diameter. When $K_n \leq 0.01$, Fick diffusion is the main diffusion mechanism; when $K_n \geq 10$, Knudsen diffusion is the main diffusion mechanism; when $0.01 < K_n < 10$, the transition diffusion is the main diffusion mechanism. In the present experiment condition, the infiltration of BN during the CVI process was controlled by the diffusion of BCl_3 [29],

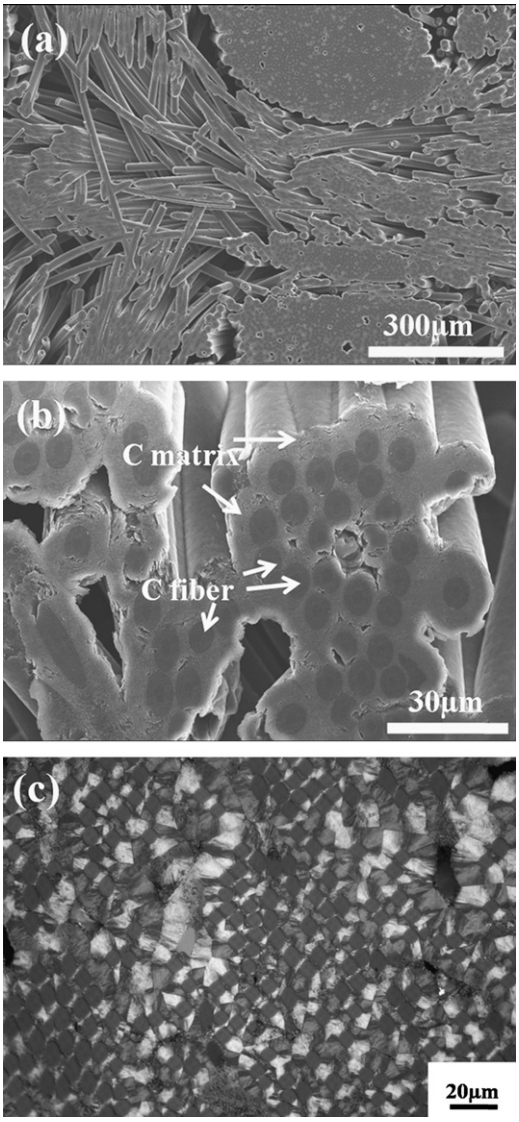

Fig. 2. Microstructure of C/C composites: (a), (b) SEM micrographs; (c) PLM micrograph.

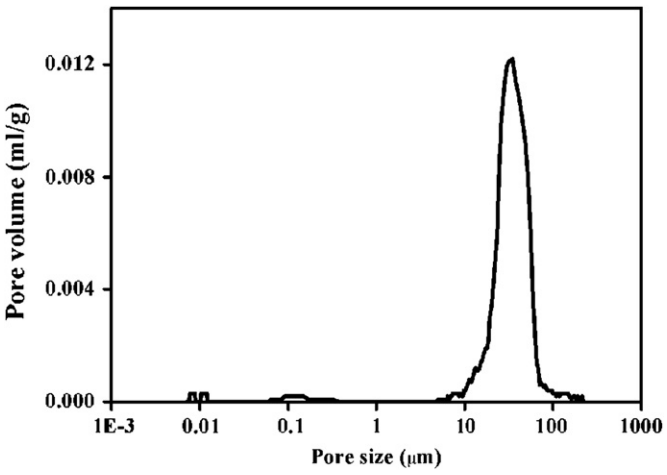

Fig. 3. Pore size distribution of C/C composites.

and the mean free path for BCl_3 was about 32 μm [35]. According to the above results, the pore size of C/C composites varied from 10 μm to 100 μm. Therefore, it can be concluded the gaseous diffusion mechanism in the C/C porous preform was the transition diffusion because the value of K_n ranged from 0.32 to 3.2 according to Eq. (2).

The smaller K_n means larger diffusion coefficient of gaseous reactants, which is beneficial to the infiltration of BN even when the competition between reaction and diffusion is considered. A measurement of competition between reaction and diffusion is the Thiele modulus (Φ) [36]:

$$\Phi = 2L\sqrt{\frac{k}{D_{eff}}dp} \tag{3}$$

where L is the length of pores, k is the heterogeneous reaction constant, D_{eff} is the effective diffusion coefficient, and d_p is the mean pore diameter. The higher Φ means the relatively quick reaction speed and the slow transfer speed of the gaseous reactants, and the reaction product was deposited near the pore entrance, leading to the formation of infiltration gradient; The smaller Φ means the quick transfer speed and the relatively slow reaction speed of gaseous reactants, and the gaseous reactants quickly diffused in the porous preform and then reacted with each other, leading to the formation of solid product homogenously distributed in the preform.

In the present experiment conditions, L and d_p were determined by the initial preform structure, k was determined by the infiltration temperature, and D_{eff} was determined by the diffusion mechanism. The transition diffusion was the main diffusion mechanism, which meant that the Knudsen diffusion and Fick diffusion existed simultaneously. The existence of Fick diffusion or near-Fick type diffusion determines the quick transfer speed of gaseous reactants during the CVI process, leading to the high D_{eff}. According to Eq. (3), the high D_{eff} leads to the low Φ, which presents the quick transfer speed and the relatively slow reaction speed of gaseous reactants. Therefore, it can be concluded that BN shows the good infiltration ability during the CVI process.

3.3. Phase composition and microstructure of C/C–BN composites

The XRD pattern of C/C–BN composites is presented in Fig. 4, which is compared with those of C/C and C/C–SiC composites. The diffraction peaks of carbon had no deviation for different composites, implying that the processing temperatures of C/C–BN composites and C/C–SiC composites had little influence on the d_{002} spacing of carbon. After heat-treated at 1600 °C, turbostratic BN matrix was transformed into hexagonal one. Therefore, there exists a diffraction peak at 2θ of about 53 ° for C/C–BN composites due to the introduction of BN. Through analyzing on the weight variation of C/C composites

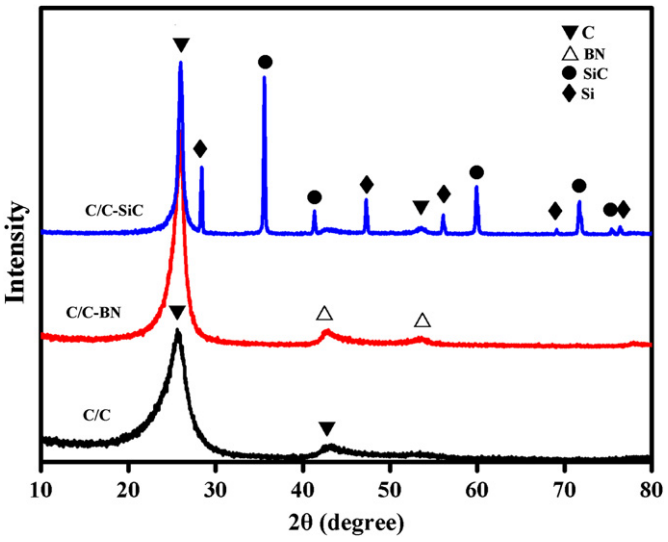

Fig. 4. XRD patterns of different composites.

during the CVI BN process, it can be known that C/C–BN composites were composed of 92 vol% C and 8 vol% BN. For C/C–SiC composites, liquid silicon was introduced into the C/C composites, and reacted with carbon matrix to form SiC matrix. In the final composites, part of silicon remained, and C/C–SiC composites were composed of carbon, SiC and silicon. The contents of carbon, silicon, and SiC in C/C–SiC composites were determined by gravimetric analysis. Silicon was removed by dissolving the composites in a mixture of hydrofluoric and nitric acid (HNO_3:HF = 4:1) for 48 h, and carbon phase was removed by burning it off at 700 °C for 20 h in air, so the residual SiC was determined. The above analysis revealed that C/C–SiC composites were composed of 70 vol% C, 22 vol% SiC and 8 vol% Si.

The density and open porosity of C/C–BN composites were 1.65 g/cm^3 and 15%, respectively. Compared to C/C composites, the increase in density and the decrease in open porosity of C/C–BN composites were attributed to the introduction of BN matrix. As shown in Fig. 5(a) and (b), BN matrix layer was formed around the carbon matrix, and BN was distributed in the inter-bundle pore and intra-bundle pore homogeneously, implying the good infiltration ability of BN in the CVI process, which was consistent with the above previous results. For C/C–SiC composites, the pores in the C/C preform were infiltrated by the liquid silicon, leading to relatively denser surface than C/C and C/C–BN composites. The density and open porosity of C/C–SiC composites were 1.90 g/cm^3 and 11%, respectively. As shown in Fig. 5(c) and (d), SiC and Si in C/C–SiC composites was mainly distributed in the short fiber web layers and the inter-bundle matrix.

3.4. Friction and wear properties

The friction and wear properties of different composites were tested at a braking speed of 28 m/s under 0.8 MPa.

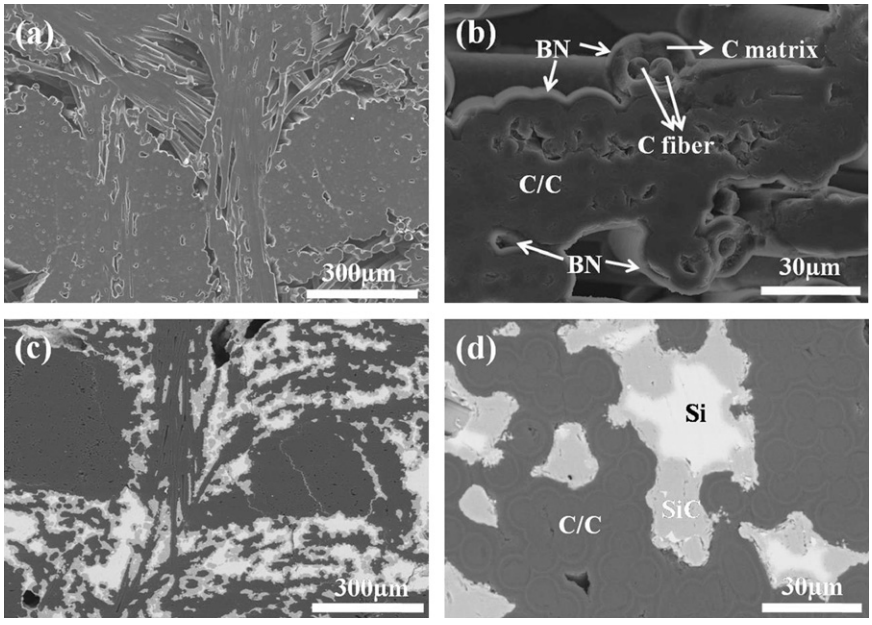

Fig. 5. SEM micrographs of different composites: (a) and (b) C/C–BN composites, (c) and (d) C/C–SiC composites.

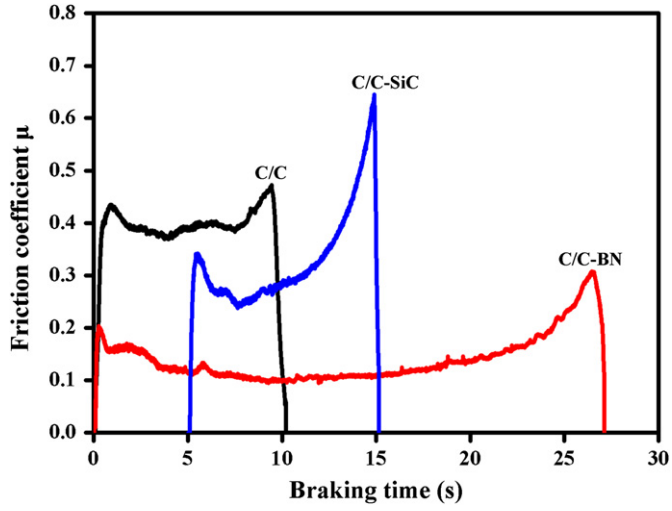

Fig. 6. Friction coefficient curves of different composites at a braking speed of 28 m/s under 0.8 MPa.

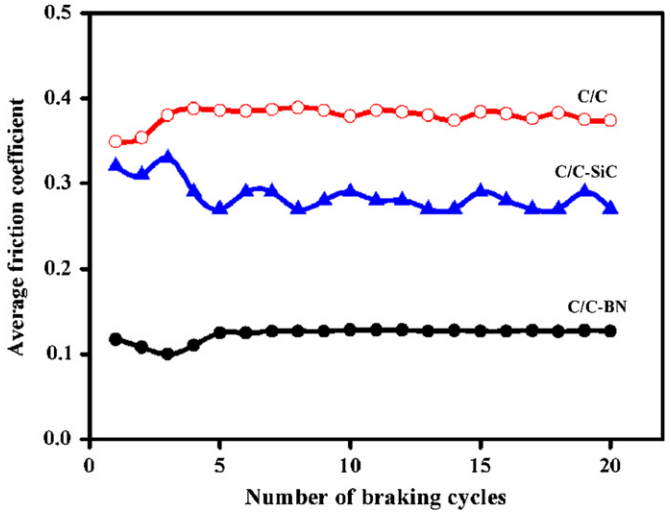

Fig. 7. Relationship of average friction coefficient and braking numbers for different composites.

Fig. 6 presents the friction coefficient curves of different composites, which all revealed a typical "saddle" shape. In comparison to C/C composites and C/C–SiC composites, C/C–BN composites showed relatively lower peak value at the beginning and end of braking, and presented a long and smooth middle stage. The friction coefficient of C/C–BN composites reached as low as 0.10, indicating the excellent lubricating performance of BN matrix.

Fig. 7 presents the variation of average friction coefficient with the braking numbers for different composites. The average friction coefficient of C/C composites, C/C–BN composites and C/C–SiC composites varied from 0.35 to 0.39, 0.11 to 0.13, and 0.27 to 0.33, respectively. The average friction coefficient of C/C–BN composites changed in a narrow range versus the braking number, which suggests a better braking stability of friction behaviors than C/C composites and C/C–SiC composites.

Table 1 lists the average friction coefficient and weight wear rate of different composites in the same test condition. The average friction coefficient of C/C composites, C/C–BN composites and C/C–SiC composites were 0.38, 0.12 and 0.29, respectively. C/C–BN composites showed the lowest average friction coefficient, which was less than one-third of C/C composites. Not only the average friction coefficient of C/C composites in this paper, but also the average friction coefficients of C/C composites in the literatures [3,37,38] were rarely less than 0.30 in the similar test condition. The weight wear rates of C/C composites,

Table 1
Comparison on the properties of C/C composites, C/C–BN composites and C/C–SiC composites.

Composites	Process	Density (g/cm^3)	Porosity (vol%)	Average friction coefficient	Weight wear rate (mg/cycle)
C/C	CVI	1.50	25	0.38	20.7
C/C–BN	CVI	1.65	15	0.12	12.8
C/C–SiC	CVI+LSI	1.90	11	0.29	16.4

C/C–BN composites and C/C–SiC composites were 20.7, 12.8 and 16.4 mg/cycle, respectively. C/C–BN composites showed the best wear resistance. In summary, the incorporation of BN was an effectively way to decrease the friction coefficient and wear rate of C/C composites.

Fig. 8 presents the friction surface morphologies of different composites. It can be found that C/C composites showed a coarser surface, while C/C–BN composites and C/C–SiC composites showed a relatively smooth friction surface after the braking test. A homogeneous friction film was formed between disks for C/C–BN composites and C/C–SiC composites. The formation of friction film was the accumulation of lots of debris on the friction surface, which was beneficial to the alleviation of the ploughing effect between two disks, leading to the improvement of the tribological properties. During the braking process, the formation of friction film was a dynamic state of balance [3]. Indeed, friction film was treated as a compacted layer between two disks [39]. The wear debris was generated constantly with the proceeding of braking, and escaped from the rubbing surface by the acentric force simultaneously. For C/C composites, wear debris filled the open pores in the matrix predominately, leading to the less accumulation on the rubbing surface. For C/C–BN composites, BN located in the wear debris between two disks during the braking process. The deformation and lubricating effect of BN alleviated the ploughing effect between two disks, which was beneficial to the formation of friction film [15]. For C/C–SiC composites, the relatively dense surface was beneficial to the large accumulation of wear debris on the rubbing surface. As shown in Fig. 9, the wear debris of C/C–BN composites and C/C–SiC composites displayed smaller size than those of C/C composites. With the formation of friction film, the ploughing effect between two disks was alleviated, and the wear debris was grinded repeatedly and then dropped from the rubbing surface, leading to the formation of the smaller debris size. Especially for the C/C–BN composites, the lower friction coefficient meant the longer braking time, implying that the wear debris was grinded between friction surfaces for longer time, leading to the appearance of the large amount of powdery debris.

Known from the above results, both C/C composites and C/C–BN composites had the same fiber preform and pyrolytic carbon matrix, and the difference of which was the existence of BN matrix for C/C–BN composites. With

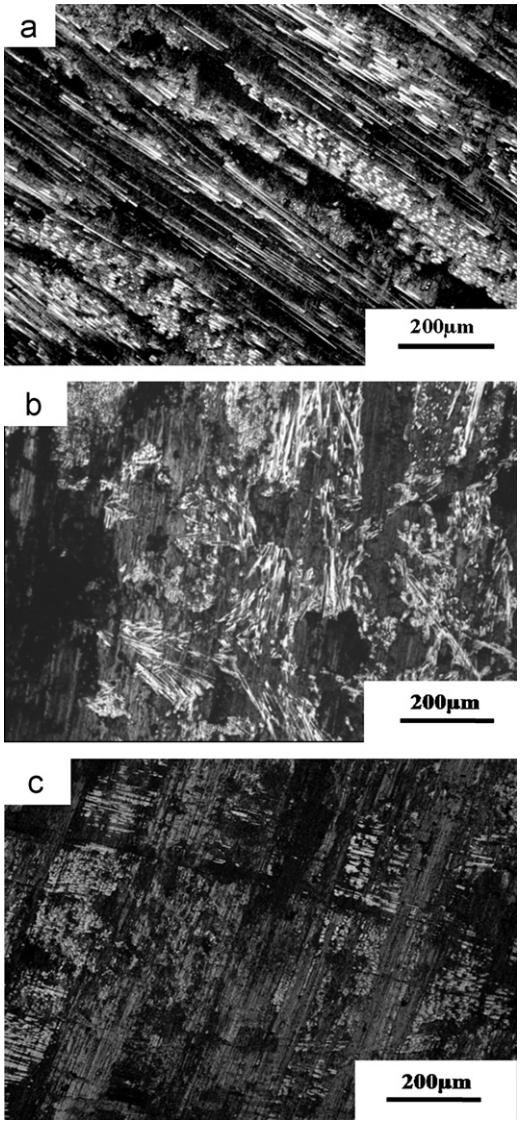

Fig. 8. Optical micrographs of friction surface for different composites after the braking test: (a) C/C composites, (b) C/C–BN composites and (c) C/C–SiC composites.

the incorporation of BN, the friction coefficient and wear rate of C/C composites decreased obviously. BN has similar laminate structure to graphite and MoS_2, and the weak bonding force between each layer makes it easily to cleavage and deform along the sliding direction, leading to the excellent lubricating performance of BN. In the braking process, the incorporation of BN in C/C composites was treated as lubricating additive existing between two disks. The mechanical action and friction force between two disks were alleviated due to the existence of solid lubricant BN, thereby decreasing the friction coefficient and wear rate. At the same time, the incorporation of BN matrix improved the oxidation resistance of C/C composites, which was beneficial to improving the wear resistance [3,25]. In the braking process, the temperature of friction surface was enough high to the onset of carbon matrix and carbon fiber. The oxidation of carbon matrix and carbon fiber closed to the friction surface would

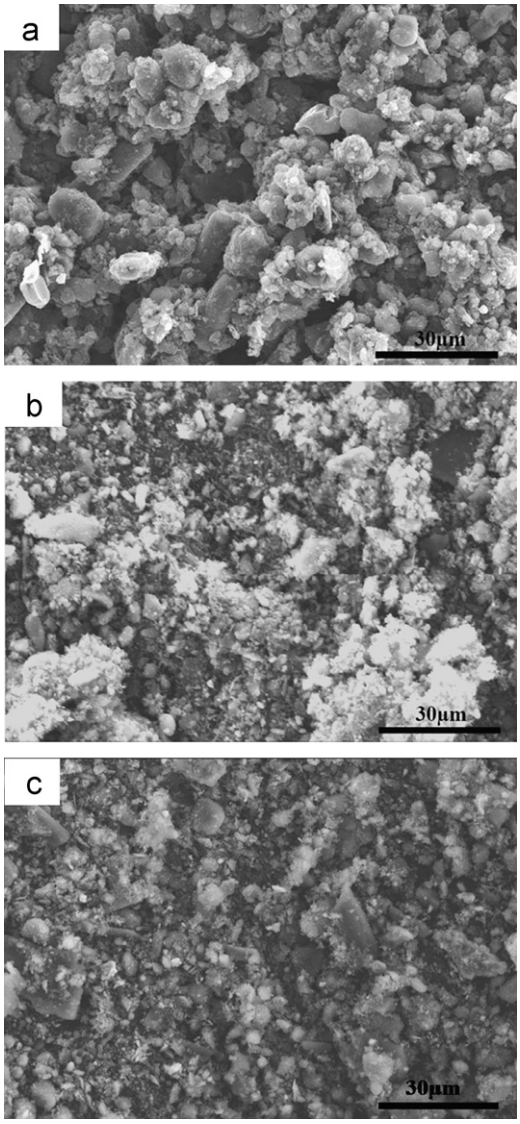

Fig. 9. SEM micrographs of the wear debris for different composites: (a) C/C composites, (b) C/C–BN composites and (c) C/C–SiC composites.

decrease the strength and weaken the load capacity, which aggravated the wear and increased the wear rate. In the braking process, the C/C–BN composites could maintain the better strength than the C/C composites owing to the better oxidation resistance of BN matrix, thereby decreasing the wear rate. Based on the above results, C/C–BN composites showed lower friction coefficient and lower wear rate than C/C composites.

4. Conclusions

(1) During the CVI BN process, the gaseous diffusion mechanism in the C/C porous preform was the transition diffusion due to the value of K_n varying from 0.32 to 3.2, leading to the quick transfer speed and the relatively slow reaction speed of gaseous reactants. Therefore, BN showed good infiltration ability in the CVI process.

(2) BN was introduced into C/C composites by CVI to fabricate C/C–BN composites. By calculating the weight variation during the CVI BN process, C/C–BN composites were composed of 92 vol% C and 8 vol% BN. The inter-bundle pore and intra-bundle pore of the porous composites was well infiltrated by the BN matrix due to the good infiltration ability of BN.

(3) Compared to C/C composites and C/C–SiC composites, C/C–BN composites showed lower friction coefficient and lower wear rate. At a braking speed of 28 m/s under 0.8 MPa, C/C–BN composites had an average friction coefficient of 0.12 and a weight wear rate of 12.8 mg/cycle. Both friction coefficient and wear rate of C/C composites decreased significantly with the incorporation of CVI BN matrix.

Acknowledgments

The authors are grateful for the supports of the Natural Science Foundation of China (Project no. 50972119), the 863 National High-tech Research Development Plan (863 plan) (Project no. 2007AA03Z542), the Projects of International Cooperation and Exchanges NSFC (Contract no. 50820145202) and the 111 Project (B08040).

References

[1] R. Weiβ, Carbon/Carbons and their industrial applications, in: W. Krenkel (Ed.), Ceramic Matrix Composites: Fiber Reinforced Ceramics and Their Applications, Wiley, Germany, 2008, pp. 69–111.
[2] B. Chen, L.T. Zhang, L.F. Cheng, X.G. Luan, Ablation of pierced C/C composite nozzles in an oxygen/ethanol combustion gas generator, Carbon 47 (2009) 545–550.
[3] X. Xiong, B.Y. Huang, J.H. Li, H.J. Xu, Friction behaviors of carbon/carbon composites with different pyrolytic carbon textures, Carbon 44 (2006) 463–467.
[4] S. Singh, V.K. Srivastava, Electrical properties of C/C and C/C–SiC ceramic fibre composites, Ceramics International 37 (2011) 93–98.
[5] J.D. Chen, J.H. Chern Lin, C.P. Ju, Effect of humidity on the tribological behavior of carbon–carbon composites, Wear 193 (1996) 38–47.
[6] R.Y. Luo, X.L. Huai, J.W. Qu, H.Y. Ding, S.H. Xu, Effect of heat treatment on the tribological behavior of 2D carbon/carbon composites, Carbon 41 (2003) 2693–2701.
[7] X.T. Shen, K.Z. Li, H.J. Li, H.Y. Du, W.F. Cao, F.T. Lan, Microstructure and ablation properties of zirconium carbide doped carbon/carbon composites, Carbon 48 (2010) 344–351.
[8] S.F. Tang, J.Y. Deng, S.J. Wang, W.C. Liu, K Yang, Ablation behaviors of ultra-high temperature ceramic composites, Materials Science and Engineering A 465 (2007) 1–7.
[9] S.J. Park, M.K. Seo, J.R. Lee, Effect of oxidation inhibitor on the low energy tribological behavior of carbon–carbon composites, Carbon 40 (2002) 835–843.
[10] C.G. Cofer, J. Economy, Oxidative and hydrolytic stability of boron nitride—a new approach to improving the oxidation resistance of carbonaceous structures, Carbon 33 (1995) 389–395.
[11] W.X. Wang, Y. Takao, T. Matsubara, Tensile strength and fracture toughness of C/C and metal infiltrated composites Si–C/C and Cu–C/C, Composites Part A 39 (2008) 231–242.

[12] W. Krenkel, B. Heidenreich, R. Renz, C/C–SiC composites for advanced friction systems, Advanced Engineering Materials 4 (2002) 427–436.
[13] S. Fouquet, M. Rollin, R. Pailler, X. Bourrat, Tribological behaviour of composites made of carbon fibres and ceramic matrix in the Si–C system, Wear 264 (2008) 850–856.
[14] S.W. Fan, L.T. Zhang, Y.D. Xu, L.F. Cheng, J.J. Lou, J.Z. Zhang, L. Yu, Microstructure and properties of 3D needle-punched carbon/silicon carbide brake materials, Composites Science and Technology 67 (2007) 2390–2398.
[15] G.P. Jiang, J.F. Yang, Y.D. Xu, J.Q. Gao, J.Z. Zhang, L.T. Zhang, L.F. Cheng, J.J. Lou, Effect of graphitization on microstructure and tribological properties of C/SiC composites prepared by reactive melt infiltration, Composites Science and Technology 68 (2008) 2468–2473.
[16] S.W. Fan, L.T. Zhang, L.F. Cheng, S.J. Yang, Microstructure and frictional properties of C/SiC brake materials with sandwich structure, Ceramics International 37 (2011) 2829–2835.
[17] X.W. Yin, S.S. He, L.T. Zhang, S.W. Fan, L.F. Cheng, G.L. Tian, T. Li, Fabrication and characterization of a carbon fibre reinforced carbon–silicon carbide–titanium silicon carbide hybrid matrix composite, Materials Science and Engineering A 527 (2010) 835–841.
[18] X.M. Fan, X.W. Yin, S.S. He, L.T. Zhang, L.F. Cheng, Friction and wear behaviors of C/C–SiC composites containing Ti_3SiC_2, Wear 274 (2012) 188–195.
[19] R. Weiss, Applications of CMCs, in: Proceedings of HTCMC-6 conference, New Delhi, September, 2007.
[20] M. Engler, C. Lesniak, R. Damasch, B. Ruisinger, J. Eichler, Hexagonal boron nitride (hBN)-applications from metallurgy to cosmetics, Cfi/Ber DKG, 84 2007. pp. 49–53.
[21] S. Rudolph, Composition and application of coatings based on Boron Nitride, Interceram 42 (1993) 302–305.
[22] R.F. Deacon, J.F. Goodman, Lubrication by lamellar solids, Proceedings of the Royal Society of London Series A 243 (1958) 464–482.
[23] W. Chen, Y.M. Gao, C. Chen, J.D. Xing, Tribological characteristics of Si_3N_4–hBN ceramic materials sliding against stainless steel without lubrication, Wear 269 (2010) 241–248.
[24] Z. Pawlak, T. Kaldonski, R. Pai, E. Bayraktar, A. Oloyede, A comparative study on the tribological behaviour of hexagonal boron nitride (h-BN) as lubricating micro-particles—an additive in porous sliding bearings for a car clutch, Wear 267 (2009) 1198–1202.
[25] S. Seghi, B. Fabio, J. Economy, Carbon/carbon–boron nitride composites with improved wear resistance compared to carbon/carbon, Carbon 42 (2004) 3043–3048.
[26] S. Seghi, J. Lee, J. Economy, High density carbon fiber/boron nitride matrix composites: fabrication of composites with exceptional wear resistance, Carbon 43 (2005) 2035–2043.
[27] R. Naslain, Design, preparation and properties of non-oxide CMCs for application in engines and nuclear reactors: an overview, Composites Science and Technology 64 (2004) 155–170.
[28] R. Naslain, A. Guette, F. Rebillat, R. Pailler, F. Langlais, X. Bourrat, Boron-bearing species in ceramic matrix composites for long-term aerospace applications, Journal of Solid State Chemistry 177 (2004) 449–456.
[29] Y. Cheng, X.W. Yin, Y.S. Liu, S.W. Li, L.F. Cheng, L.T. Zhang, BN coatings prepared by low pressure chemical vapor deposition using boron trichloride–ammonia–hydrogen–argon mixture gases, Surface and Coatings Technology 204 (2010) 2797–2802.
[30] J.G. Li, H. Hausner, Reactive wetting in the liquid-silicon/solid-carbon system, Journal of the American Ceramic Society 79 (1996) 873–880.
[31] H. Zhou, R.N. Singh, Kinetic model for the growth of silicon carbide by the reaction of liquid silicon with carbon, Journal of the American Ceramic Society 78 (1995) 2456–2462.
[32] X.W. Yin, L.F. Cheng, L.T. Zhang, Y.D. Xu, C. You, Microstructure and oxidation resistance of carbon/silicon carbide composites infiltrated with chromium silicide, Materials Science and Engineering A 290 (2000) 89–94.
[33] H.J. Li, X.H. Hou, Y.X. Chen, Densification of unidirectional carbon–carbon composites by isothermal chemical vapor infiltration, Carbon 38 (2000) 423–427.
[34] P. Delhaes, Chemical vapor deposition and infiltration processes of carbon materials, Carbon 40 (2002) 641–657.
[35] Y.S. Liu, L.F. Cheng, L.T. Zhang, Y.F. Hua, W.B. Yang, Microstructure and properties of particle reinforced silicon carbide and silicon nitride ceramic matrix composites prepared by chemical vapor infiltration, Materials Science and Engineering A 475 (2008) 217–233.
[36] J.S. Li, R.Y. Luo, Kinetics of chemical vapor infiltration of carbon nanofiber-reinforced carbon/carbon composites, Materials Science and Engineering A 480 (2008) 253–258.
[37] X. Xiong, J.H. Li, B.Y. Huang, Impact of brake pressure on the friction and wear of carbon/carbon composites, Carbon 45 (2007) 2692–2694.
[38] H.L. Deng, K.Z. Li, H.J. Li, P.Y. Wang, J. Xie, L.L. Zhang, Effect of brake pressure and brake speed on the tribological properties of carbon/carbon composites with different pyrocarbon textures, Wear 270 (2010) 95–103.
[39] J.R. Jiang, F.H. Stott, M.M. Stack, A generic model for dry sliding wear of metals at elevated temperatures, Wear 256 (2004) 973–985.